Journal of Chromatography A, 662 (1994) 153–166
Elsevier Science B.V., Amsterdam

CHROM. 25 692

System peaks and disturbances to the baseline UV signal in capillary zone electrophoresis

J.L. Beckers

Laboratory of Instrumental Analysis, Eindhoven University of Technology, P.O. Box 513, 5600 MB Eindhoven (Netherlands)

(Received September 15th, 1993)

ABSTRACT

Non-steady-state processes in capillary electrophoresis can be estimated by applying a steady-state mathematical model. Calculations with a steady-state model indicate that in capillary electrophoresis, moving boundary zones can originate from discontinuities in the concentration of the co-ions and/or the pH of the background electrolyte. Calculations showed that cationic moving boundaries with high mobilities originate with low system pH values. If the separation capillary and anode compartment are filled with electrolytes, different in concentration or pH, a shift of the baseline UV signal can occur. Block-shaped discontinuities in pH and/or concentrations split up in a migrating part with a mobility determined by the composition of the background electrolyte and a part migrating with the velocity of the electroosmotic flow at the position of the original disturbance. As a result, dips of the electroosmotic flow marker (low background concentration) split up and a negative system peak migrates through the system at low system pH values. Injections of high concentrations of background electrolyte or samples at high ionic strength lead to positive system peaks. These system peaks are, of course, only visible if the background electrolyte shows UV-absorbing properties. Experimentally determined data match the calculated values for these mobilities and baseline shifts.

INTRODUCTION

In the performance of electrophoretic experiments, mixed-mode effects can often be observed. In capillary zone elecrophoresis (CZE), *e.g.*, isotachophoretic (ITP) effects can act, and a specific choice of the electrolyte systems results in, *e.g.*, on-column transient and coupled column ITP preconcentration [1,2] and ITP/CZE [3]. Also other curious phenomena, linked with pH and concentration disturbances, are evident in CZE. Because UV detectors are often applied in CZE, phenomena related to concentration disturbances are only observable on applying background electrolytes with UV-absorbing properties (indirect UV mode). Often pH and concentration disturbances originate from a different composition of the electrolytes in the capillary and electrode compartments and cause system peaks, baseline shifts and unstable baselines. Vinther *et al.* [4] observed a jump in the baseline UV absorbance signal from one stable level to another at the position of the electroosmotic flow (EOF) marker. Beckers and Ackermans [5] reported a reversed migration behaviour due to pH disturbances in CZE as a result of an imbalance of the hydrogen mass balance. Disturbances by an imbalance of the hydrogen mass balance can be expected on applying background electrolytes at low or high pH. In this paper, the presence of system peaks and shifts in the baseline of the UV signal originating from discontinuities in pH and concentration of the co-ions in background electrolytes are discussed.

EXPERIMENTAL

For all CZE experiments, a P/ACE System 2000 HPCE instrument (Beckman, Palo Alto, CA, USA) was used. All experiments were carried out applying a Beckman eCAP capillary tubing (75 μm I.D.) with a total length of 46.7

0021-9673/94/$07.00
SSDI 0021-9673(93)E1150-X

cm and a distance between injection and detection of 40.0 cm. The wavelength of the UV detector was set at 214 nm. The operating temperature was 25°C and all experiments were carried out applying 15 kV, unless stated otherwise. Sample injection was performed by applying pressure injection where a 1-s pressure injection equals an injection amount of *ca.* 6 nl and an injected length of 0.136 cm. Data analysis was performed using the laboratory-written data analysis program CAESAR.

RESULTS AND DISCUSSION

System peaks

In CZE experiments, in the indirect UV mode, peaks of the electrosmotic flow marker split up on applying background electrolytes at low pH and a system peak appears. As an example, in Fig. 1A the electropherogram is given of the separation of the 5-s pressure injection of a mixture of 0.0001 *M* potassium, sodium, tetramethyl- (TMA), tetraethyl-(TEA) and tetrabutylammonium (TBA) ions applying a background electrolyte of 0.005 *M* histidine adjusted to pH 5.0 by adding formic acid. The system peak (sharp at the front and diffuse at the rear) is also present on injecting pure water (see Fig. 1B). Such a system peak can be characterized by a mobility with a value determined by the composition of the background electrolyte. In Fig. 2, some electropherograms are given 5-s pressure injections of pure water applying background electrolytes of 0.01 *M* histidine adjusted to different pHs by adding acetic acid. It can be seen that the mobilities of the system peaks increase at low pH. To demonstrate the effect of the composition of the injected solution, in Fig. 3 the electropherograms are given for 5-s pressure injections of several dilutions of the background elecrolyte 0.01 *M* histidine adjusted to pH 3.8 by adding formic acid. The system and the EOF peaks are always present on injecting dilute background electrolytes, whereas on injecting pure background electrolytes small baseline disturbances mark the positions of these peaks. Although the migration times of the peaks can vary, owing to varying mobilities of

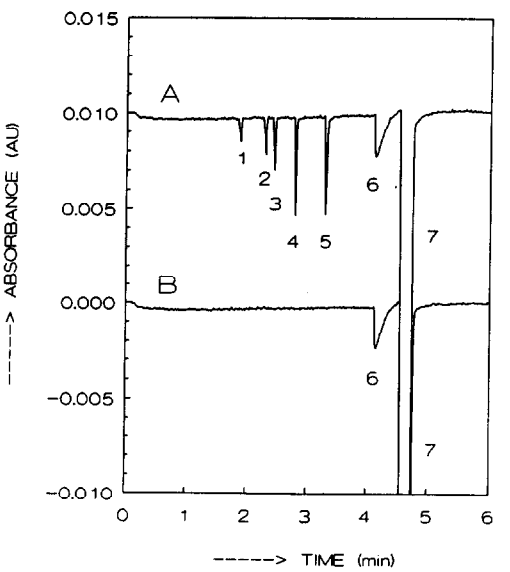

Fig. 1. Electropherograms of (A) the separation of the 5-s pressure injection of a mixture of 0.0001 *M* (1) potassium, (2) sodium, (3) tetramethyl-, (4) tetraethyl- and (5) tetrabutylammonium ions and (B) the 5-s pressure injection of pure water, applying a background electrolyte of 0.005 *M* histidine adjusted to pH 5.0 by adding formic acid. The EOF peak (7) splits up and a system peak (6) appears.

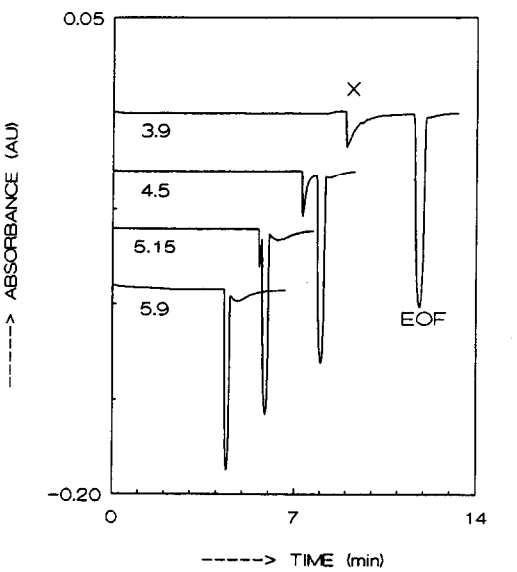

Fig. 2. Electropherograms for 5-s pressure injections of water in background electrolytes of 0.01 *M* histidine adjusted to different pHs by adding acetic acid. The numbers refer to the pH of the background electrolyte solutions. System peaks X show higher and EOF peaks show lower mobilities at lower pH.

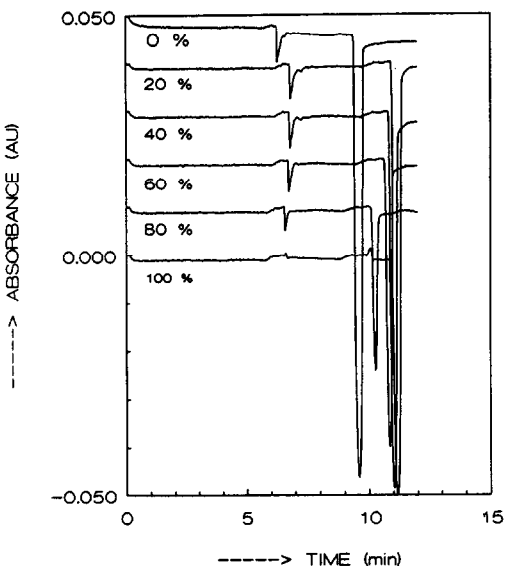

Fig. 3. Electropherograms for 5-s pressure injections of several dilutions of background electrolyte. The percentages are the concentrations of background electrolyte used for the injection. The background was 0.01 *M* histidine adjusted to pH 3.8 by adding formic acid.

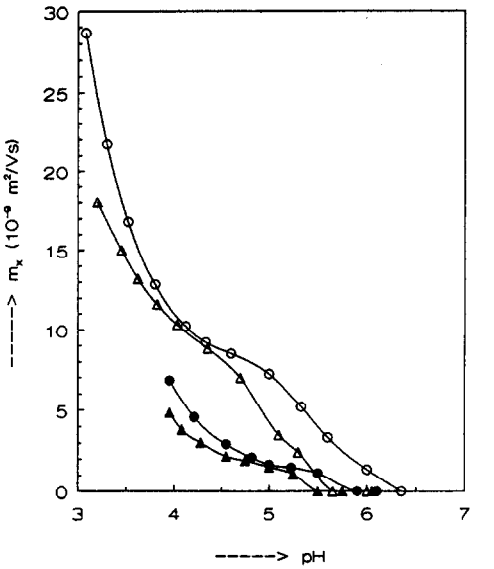

Fig. 4. Measured mobilities of system peaks X as function of the pH of background electrolytes consisting of 0.01 *M* imidazole with the pH adjusted by adding (○) formic acid and (●) acetic acid and of 0.01 *M* histidine with the pH adjusted by adding (△) formic acid and (▲) acetic acid.

the EOF, the mobilities of the system peaks were constant. In Fig. 4 the measured mobilities of the system peaks, for 5-s pressure injections of water, are given for background electrolytes of 0.01 *M* histidine and 0.01 *M* imidazole adjusted to different pH values by adding formic and acetic acid. The mobilities increase at lower pH and with formic acid. On applying background electrolytes without UV-absorbing properties such as 0.01 *M* potassium formate and acetate at different pHs, such system peaks cannot be observed.

In ITP experiments hydrogen ions can act as a terminator [6–8]. Sharp zone boundaries are typical for ITP zones. Because the system peaks are sharp at the front and diffuse at the rear, in the first instance the origin of these peaks was ascribed to a local disturbance of the zone electrophoretic process and a local ITP terminating effect was assumed. With a mathematical, model, described previously [8], the mobilities of terminating hydrogen zones for the electrolyte systems used in Fig. 4 were calculated. In Fig. 5 the calculated mobilities of the terminating hydrogen zones are given and it can be concluded

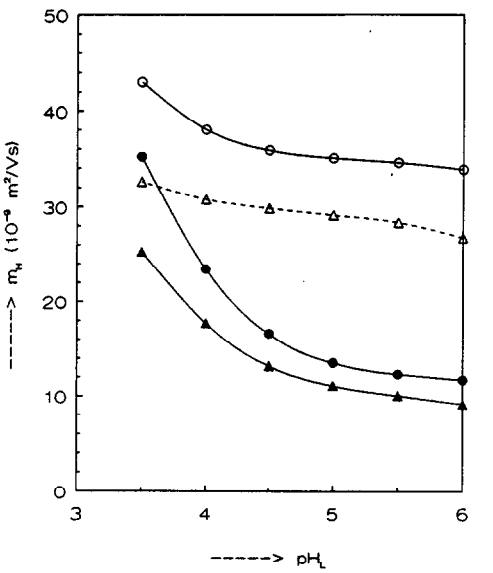

Fig. 5. Calculated mobilities of terminating hydrogen zones in ITP as function of the pH of the leading electrolyte for the systems used in Fig. 4. The dashed line indicates a non-steady-state ITP.

that these values are much higher than those of the measured system peaks from Fig. 4, indicating that the system peaks are caused by another effect.

Disturbances to baseline UV signal

Because the system peaks are only present at low pHs of the background electrolytes and their mobilities increase at lower pH, we thought that the system peaks were related to a pH shift migrating through the capillary. To study the effect of a pH shift, electropherograms were measured on applying a background electrolyte at the inlet side (anode) consisting of the same concentration of the cationic species in the separation capillary but at a different pH. In Fig. 6 the electropherograms are given for 5-s pressure injections of water, filling the cathode compartment and capillary with the background electrolyte 0.01 *M* histidine adjusted to pH 3.8 by adding formic acid and filling the anode compartment (inlet side) with 0.01 *M* histidine adjusted to different pHs by adding formic acid. Surprisingly, diffuse disturbances of the baseline were present, between the system peaks X as described earlier (and with the same mobility) and the EOF marker. The UV absorbances of the leading and terminating electrolytes are nearly equal. Without the injection of water the dip of the system peak disappeared, but the shift of the baseline started at the same position. The migration times of the system and EOF peaks differ for larger differences between the pHs of electrolytes in the separation capillary and anode compartment, because the mobility of the EOF of the electrolyte in the anode compartment is higher, ultimately resulting in a higher overall EOF in the separation capillary. The disturbance to the baseline (increase in UV signal) is stronger for larger differences in pH of the electrolytes in the capillary and anode compartment. Because the measurements show that the UV absorbances for equimolar solutions of histidine at different pHs between 3 to 6 are nearly equal, the increase in the UV signal of the baseline must be caused by an increase in the concentration of histidine. This means that on applying electrolytes at different pH values ($pH_L < pH_T$) in the capillary and anode compartment a diffuse zone of increasing concentration of histidine appears between the position of the system peak and the EOF marker.

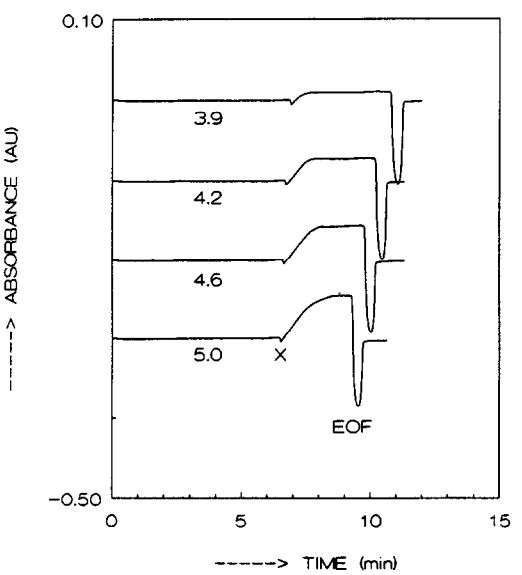

Fig. 6. Electropherograms for 5-s pressure injections of water, filling the cathode compartment and separation capillary with the background electrolyte of 0.01 *M* histidine adjusted to pH 3.8 by adding formic acid and filling the anode compartment (inlet side) with 0.01 *M* histidine adjusted to different pHs by adding formic acid. The numbers refer to the pH in the anode compartment. Shifts in baseline UV signal are obtained from the position of system peaks X to EOF marker.

Mathematical model

The electrophoretic separation mechanism can approximately be described by Kohlrausch's regulation function, originally derived for strong monovalent ions [9]. Dismukes and Alberty [10] showed that this regulating function also can be applied for weak monovalent ionic species and is often applied for electrophoretic calculations in the form

$$\sum_i \frac{\bar{c}_i}{m_i} = \omega \qquad (1)$$

where $\bar{c}_i$ and m_i represent the total concentrations and absolute values of the effective ionic mobilities of all components present in the electrolyte solution and the numerical value of the Kohlrausch's function ω is locally invariant with time [11], under certain conditions.

In isotachophoresis, sample components are separated using a leading and terminating electrolyte and the application of Kohlrausch's law gives, for strong monovalent ionic species,

$$c_A = c_L \cdot \frac{m_A(m_L + m_C)}{m_L(m_A + m_C)} \quad (2)$$

where c and m represent the ionic concentrations and absolute values of the ionic mobilities of the sample component A, leading ions L and buffering counter ions C.

Often a steady-state model [8], including corrections for the effect of pH and relaxation and retardation effects on the mobilities, is used and generally four equations are needed to calculate all parameters of the zones, *viz.*, the modified Ohm's law, the buffer balance, the electroneutrality equation (EN) and the isotachophoretic condition (IC). In such a model it is assumed that all parameters of the proceeding zones are determined by the composition of the leading electrolyte, via the buffer balance and isotachophoretic condition. Original compositions of terminating and sample solutions are of no importance. Applying the steady-state model, Kohlrausch's law is implicitly obeyed and ω values are fairly constant for all zones both for cationic and anionic systems.

Considering the electrophoretic experiments in Fig. 6, where the separation capillary is filled with a leading electrolyte L and the anode compartment with a terminating electrolyte T, consisting of the leading ion at the same concentration but at a higher pH (see Fig. 7), an adapted zone L′ should be formed between the zones T and L with exactly the same composition as L, applying the steady-state model for ITP, *i.e.*, the shift of the baseline of the UV signal cannot be explained with the steady-state model. Also, the application of Kohlrausch's law, under the assumption that the pH in zone L′ is high (a low hydrogen concentration), resulting in a small increase in the concentration of histidine, cannot explain the large increase in histidine concentration.

However, the increase in histidine concentration in the extra zone X can be fairly easily explained. The contribution of the hydrogen ions

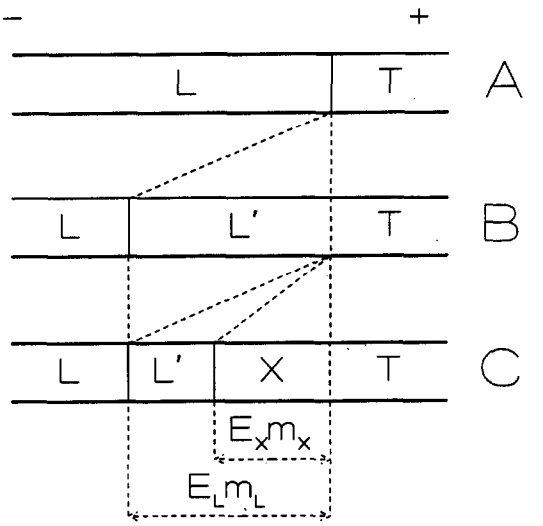

Fig. 7. (A) If the cathode compartment and the separation capillary are filled with a leading electrolyte L and the anode compartment with a terminating electrolyte T with the same co-ion at the same concentration but at a higher pH, (B) an adapted zone L′ with a composition identical with that of the leading electrolyte L should be formed between the leading and terminating zones, according to the steady-state model in ITP. (C) In practice, an extra zone X at higher concentration is formed if there is an imbalance between the mass transport of the co-ions between the leading and terminating zones due to a large difference in pH.

in zone T to the conductivity is much smaller than that in zone L and because the ionic concentrations of histidine and counter ions are nearly constant, the zone resistance and hence the electric field strength E are higher in zone T. Therefore, the amount of histidine coming from zone T is higher than needed to substitute the histidine ions of the moving zone L and an extra zone X at higher histidine concentration is created (see Fig. 7C). This zone X can be characterized by a mobility m_X depending on several parameters. From the experiments it appeared that the value of m_X is smaller than that of m_L, therefore it is assumed in the model that the moving zone L is partly elongated with a zone L′ with the same composition as that of zone L and partly substituted by zone X.

In the first instance, a steady-state model was set up for the calculation of the parameters of zone X. The reduced number of parameters is five for zone X, *viz.*, the total concentrations of the histidine and counter ions, E, pH and m_X.

The equations are the EN, modified Ohm's law and the mass balances of histidine, counter ions and hydrogen ions. Calculations with this model did not give significant results. Because the length of zone X increases with time and can be very long, it is unlikely that a surplus of histidine at the T side will influence the mobility of zone X at the L side. Therefore, a model was set up with the same five parameters, but not handling mass balances over the whole of zone X but only over the front side of zone X and assuming that the X–T boundary is a concentration boundary. Also with this model it was not possible to satisfy the hydrogen balance. Bearing in mind that also in the steady-state calculation of ITP the mass balance of the hydrogen ions is not used, the parameters of zone X are approximately calculated in the following way. The total concentration of histidine is assumed in zone X, through which the unknown parameters are only four, *viz.*, the total concentration of the counter ions, pH, m_X and the E gradient. For the calculation of these parameters the mass balances of the buffer and the co-ions, the modified Ohm's law and the EN are used. The mass balance of the hydrogen ions was not taken into account. In the calculations the following equations are used.

Mass balance of the co-ions. For the derivation of the mass balance only the effect in front of zone X is taken into account (see Fig. 8A) and the equations are given for two adjacent zones with total concentrations of the co-ions A of $\bar{c}_{A,L}$ and $\bar{c}_{A,X}$, respectively. The zone boundary z is assumed to move over a distance $E_X m_X$ in unit time. Co-ions A at time $t = 0$ present at point 1 will just reach the boundary z at time $t = 1$ and move a distance $E_X m_{A,X}$. Co-ions A at time $t = 0$ present at the zone boundary z will reach point 2 at $t = 1$ and migrate a distance $E_L m_{A,L}$. The amount of co-ions A present between point 1 and zone boundary z in zone X, at $t = 0$ (amount Q_1) will be present in zone L at $t = 1$ between the zone boundary z and point 2 (Q_2). The mass balance of the co-ions A will therefore be

$$(E_X m_{A,X} - E_X m_X)\bar{c}_{A,X} = (E_L m_{A,L} - E_X m_X)\bar{c}_{A,L} \quad (3)$$

Mass balance of the counter ions C. The migration paths for the counter ions C are given in Fig. 8B. Counter ions C present at $t = 0$ at point 3 will just reach the zone boundary z at $t = 1$ and the counter ions C present at the zone boundary z at $t = 0$ will reach point 4 at $t = 1$. The migration distances are $E_L m_{C,L}$ and $E_X m_{C,X}$, respectively. The amount of counter ions C between point 3 and z in zone L at $t = 0$ (Q_1) will be present between z and point 4 in zone x at $t = 1$ (Q_2) and the mass balance of the counter ions C will therefore be

$$(E_L m_{C,L} + E_X m_X)\bar{c}_{C,L} = (E_X m_X + E_X m_{C,X})\bar{c}_{C,X} \quad (4)$$

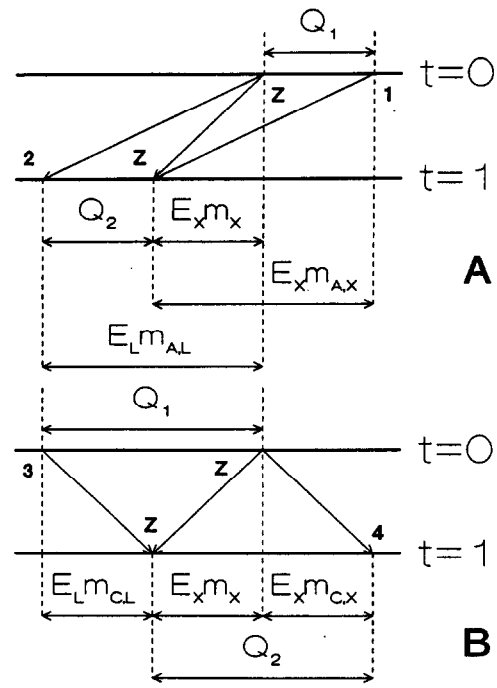

Fig. 8. Migration paths for (A) co-ions A and (B) counter ions C over a zone boundary z between leading zone L and zone X. For further explanation, see text.

The principle of electroneutrality. In accordance with the principle of electroneutrality, the arithmetic sum of all products of the concentration of all forms for all species and the corresponding valences, present in each zone, much be zero [8].

Modified Ohm's law. According to Ohm's law, the product of E and σ must be constant for all zones. The overall electrical conductivity, σ,

of a zone is the sum of the values $c|mz|F$, where z and F represent the valency of the ionic species and Faraday constant.

Procedure of calculation. The parameters of zone X are calculated in the following way. The concentration $\bar{c}_{A,X}$ is assumed. Then a pH is taken whereby all effective mobilities can be calculated and with the EN the total concentration of the counter ions $\bar{c}_{C,X}$ can be found. The zone conductivity can be calculated and with Ohm's law E can be obtained. With the mass balance of the co-ions A a value for m_X can be calculated and also with the mass balance of the counter ions C an m_X value can be obtained. For the correct pH the m_X values must be identical.

Significance of the model. In Fig. 9 the values of m_X and the ratio E_X/E_B of the electric field strengths in zone X and the background electrolyte B (right-hand scale), calculated with this model, are given as function of assumed $c_{HIST,X}$ values varying from 0.005 to 0.007 M histidine for a background electrolyte consisting of 0.006 M histidine adjusted to pH 3.5 by adding formic acid. From Fig. 9 some interesting conclusions can be drawn. If in the background electrolyte a

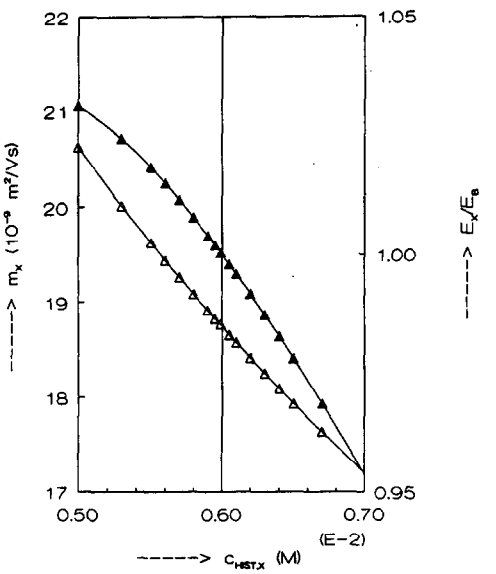

Fig. 9. Calculated values of (△) m_X of the zone X and (▲) ratio of the electric field strengths of zone X and of the background electrolyte, E_x/E_B (right-hand scale), as a function of the assumed concentration of histidine, $c_{HIST,X}$, in zone X, applying a background electrolyte consisting of 0.006 M histidine adjusted to pH 3.5 by adding formic acid. For further explanation, see text.

zone is present where the co-ions have a concentration different from that of the background electrolyte, this concentration disturbance migrates through the system with a specific mobility m_X. Note that this means that the ω value according to Kohlrausch's law is locally not invariant with time. The mobilities m_X of zones with concentrations lower than that of the background electrolyte are higher than those of zones with higher concentrations. For lower concentrations the E gradient is higher than E_B and for high concentrations it is lower. This means that zones with lower concentrations will move showing a sharp step in front of the disturbance (usually with a lower UV absorbance than the background electrolyte, because its concentration is lower), whereas disturbances at higher concentrations will be diffuse. Further, the mobilities m_X decrease for increasing concentrations. Hence the diffuse fronts in Fig. 6 can be explained. The extra zone X is not block-shaped, but diffuse at the front, through which a steady-state model over the whole zone is not significant. To calculate the shift of the baseline, zone X is thought to be built up of small steps of increasing concentrations of histidine (see Fig. 10). The mathematical model was applied in the following way. In first instance a very small increase in concentration $\bar{c}_{A,X}$ was assumed and this zone was calculated using the parameters from the background electrolyte. Then calculations were carried out whereby concentrations steps were related to the parameters of the preceding zones. These calculations were repeated until zone X, whereby

$$E_X m_{A,X} \bar{c}_{A,X} = E_T m_{A,T} \bar{c}_{A,T} \quad (5)$$

because a concentration boundary between the rear of the concentration disturbance and the terminating electrolyte is assumed.

Check of the model. To compare calculated and experimentally obtained values, concentrations must be deduced from measured steps in the UV signal. Therefore, in the first instance the UV absorbances were measured for several background electrolytes at different concentrations and different pHs. As an example, in Fig. 11 the relationship is given between the measured UV absorbances and the concentrations of solutions

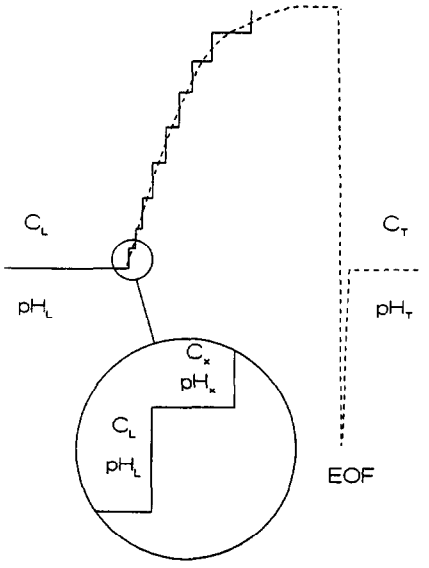

Fig. 10. For the calculation of the diffuse front of the disturbance of the baseline UV signal the shift in the baseline is thought to be built up of small steps of increasing concentrations of histidine. Calculations are started from the leading zone with a concentration c_L and pH_L. For each step the total concentration of histidine, c_X, is assumed and the other parameters are calculated using the given mathematical model.

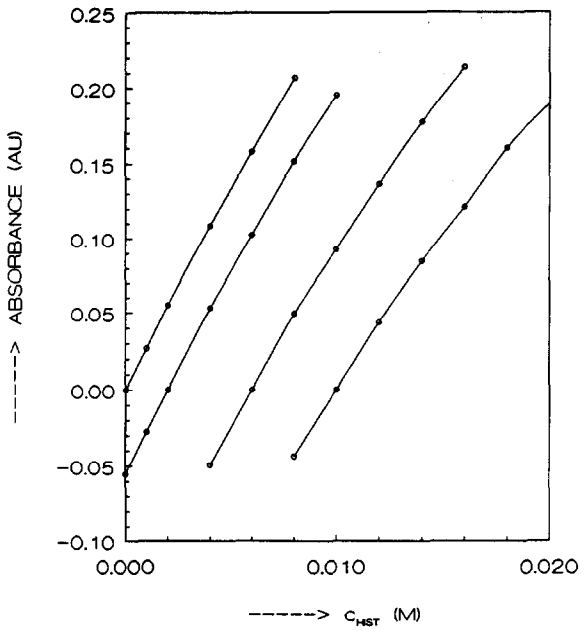

Fig. 11. Measured UV absorbances for several solutions of histidine adjusted to pH 4 by adding formic acid. Different curves were measured using different solutions for the zero setting of the UV detector. The relationships are not completely linear and the measured values differ slightly depending on the choice of the solution used for the zero setting of the UV detector.

of histidine adjusted to pH 4 by adding formic acid. Because the relationship is not completely linear and the measured values differ slightly, depending to the choice of the solution used for the zero setting of the UV detector, the relationship between absorbance and concentration is always applied using the same electrolyte for zero setting in both the calibration graph and electrophoretic experiments. From the calibration graph, shifts in the UV signal can be recalculated to concentration differences. In Fig. 12 the measured UV signals (lines) are given for leading and terminating electrolytes consisting of 0.006 *M* histidine at (A) pH 3.5 and 4, respectively, and (B) at pH 3.5 and 4.5, respectively, and the calculated values (Δ) for the concentrations, recalculated to UV values using Fig. 11. In the calculations the m_{EOF} values calculated from the experimental results are used. In practice, the m_{EOF} is not constant in such systems and the m_{EOF} is, in the first instance, determined by the composition of the leading electrolyte (low pH, low m_{EOF} value) whereas during the analysis the m_{EOF} increases because the terminating electrolyte (high pH, high m_{EOF} value) is migrating into the separation capillary. This means that in the calculations the m_{EOF} values are too high at the beginning of the analysis, through which the calculated migration times are too low, as can be seen in Fig. 12. Nevertheless, the calculations seem to be a good approximation of the measured values.

As a second check of the model, in Fig. 13 the calculated m_X values for (A) 0.01 *M* histidine and (B) 0.006 *M* histidine adjusted to different pHs by adding formic acid (lines) are compared with the measured values. The measured values were calculated from the negative dip in the UV signal applying 5-s pressure injections of water. According to the theory, these values are slightly too high, through which the measured values are higher than the calculated values, but the measured values fit the calculated lines. As a third check, calculated values of the maximum concentration of the diffuse UV signal shifts were

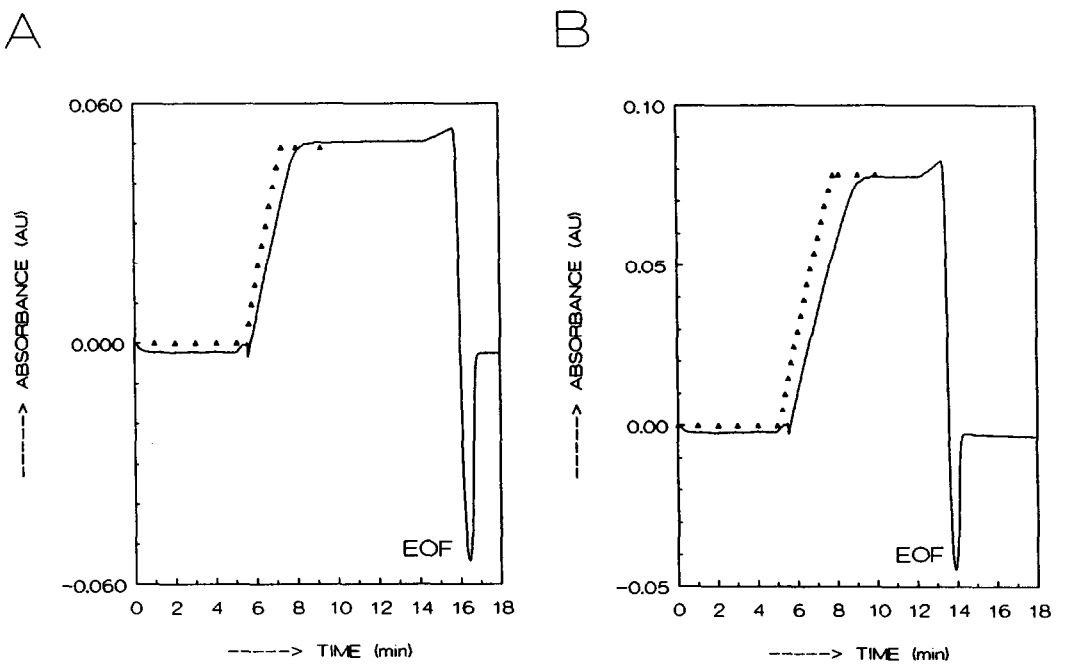

Fig. 12. Measured UV signals (lines) for leading and terminating electrolytes consisting of 0.006 *M* histidine at (A) pH 3.5 and 4, respectively, and (B) pH of 3.5 and 4.5, respectively, and (△) calculated values for the concentrations, recalculated to UV values using Fig. 11. In the calculations the m_{EOF} values calculated from the experimental results were used (applied voltage 20 kV).

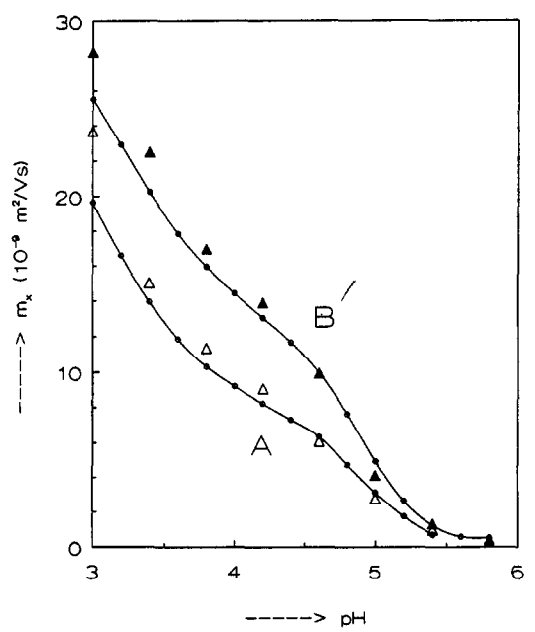

Fig. 13. Calculated (○) m_X values and measured values for (A) 0.01 *M* histidine and (B) 0.006 *M* histidine adjusted to different pHs by adding formic acid. The measured values were calculated from the negative dip in the UV signal applying 5-s pressure injections of water.

compared with measured values for several systems of histidine adjusted to pH 3.5 for the leading electrolyte by adding formic acid and to pH (A) 5, (B) 4.5 and (C) 4 for the terminating electrolyte for several concentrations of histidine. The measured UV shifts were recalculated to concentrations using Fig. 11. In Fig. 14, the calculated values (lines) and measured values are given. The calculated and measured values agree well although both the calculated and measured values increase strongly for high concentrations of histidine and a large difference between the pHs of the leading and terminating electrolyte. In that case no steady state is reached.

Moving boundary zones in LT systems. On applying in electrophoresis a terminating electrolyte, different in pH or concentration of the co-ions of the leading electrolyte, an extra zone X can be obtained migrating with a mobility m_X, determined by the composition of the leading electrolyte. In fact, a moving boundary zone is created. If the supply of co-ions coming from the terminating solution is larger than needed to

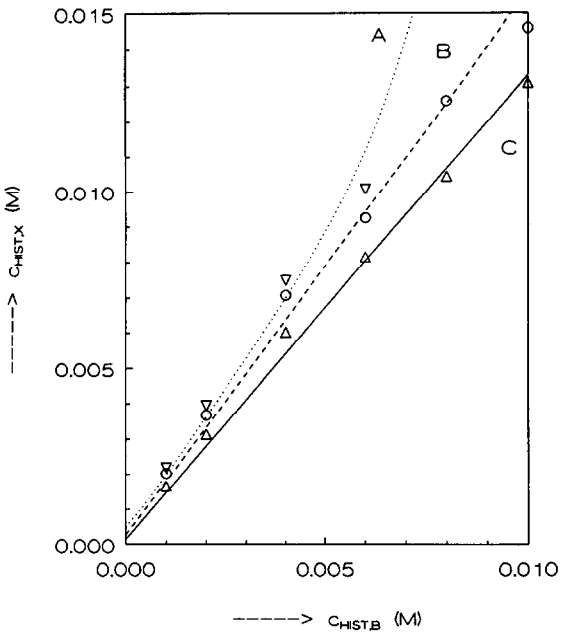

Fig. 14. Calculated values (lines) and measured values for shifts in concentrations ($c_{HIST,X}$) due to the fact that the capillary and anode compartment are filled with background electrolytes of the same concentration of histidine ($c_{HIST,B}$) but at different pH. In all experiments the leading electrolyte was at pH 3.5, whereas the pH of the terminating electrolyte was (A) 5.0 (measured values ▽), (B) 4.5 (○) and (C) 4.0 (△).

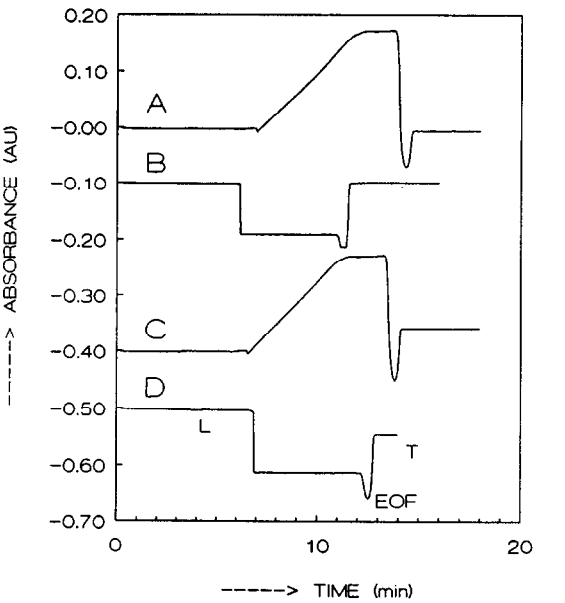

Fig. 15. Electropherograms for moving boundary zones in electrophoresis. In all instances the leading and terminating electrolytes were solutions of histidine formate. The concentrations and pH of the leading electrolytes were respectively (A) 0.01 *M* and pH 3.25, (B) 0.01 *M* and pH 4.8, (C) 0.01 *M* and pH 3.25 and (D) 0.012 *M* and pH 4.8 and in the terminating zone (A) 0.01 *M* and pH 4.8, (B) 0.01 *M* and pH 3.25, (C) 0.012 *M* and pH 4.8 and (D) 0.01 *M* and pH 3.25. For further explanation, see text.

substitute the moving co-ions of the leading electrolyte, a diffuse zone at a higher co-ion concentration than that of the leading electrolyte is obtained. If the supply is smaller, a sharp zone at lower concentration is obtained. To illustrate these effects, in Fig. 15 some of these moving boundary zones are shown. In all instances the terminating and leading electrolyte were solutions of histidine formate.

In Fig. 15A the electropherogram is given for a leading electrolyte of 0.01 *M* at pH 3.25 and a terminating electrolyte of 0.01 *M* at pH 4.8. Because the *E* gradient in the terminating zone is large compared with that in the leading zone, owing to the small contribution to the conductivity of the hydrogen ions, the supply of histidine from the terminating zone is high and a diffuse moving boundary zone can be observed. Note the small dip in front of the moving boundary zone originating from the EOF dip. The UV absorbances in the leading and terminating electrolytes are nearly equal. In Fig. 15B the concentrations and pH of the histidine formate were respectively 0.01 *M* and 4.8 in the leading zone and 0.01 *M* and 3.25 in the terminating zone. Because the supply of histidine from the terminating electrolyte is much too small, a large, sharp moving boundary zone at a lower concentration than that of the leading electrolyte migrates in front of the EOF dip. The UV signals of the leading and terminating zones are equal again. In Fig. 15C the leading electrolyte was 0.01 *M* histidine formate at pH 3.25 and the terminating electrolyte was 0.012 *M* histidine formate at pH 4.8. Analogously to Fig. 15A, a diffuse moving boundary zone is present coming to a steady state (flat profile). In Fig. 15D the leading electrolyte was 0.012 *M* at pH 4.8 and the terminating electrolyte 0.01 *M* at pH 3.25. The UV absorbance of the terminating

electrolyte is lower than that of the leading electrolyte and is preceded by a large dip of a sharp moving boundary zone.

It is clear that the use of electrolytes at different pHs or concentrations must be handled carefully, because it can result in moving boundary zones with different pHs and concentrations, not observable if the background electrolytes do not have UV-absorbing properties.

Block-shaped discontinuities in composition of background electrolytes. If a block-shaped discontinuity in pH and/or concentration of the co-ions of the background electrolytes is introduced, a steady-state discontinuity could be expected according to the simplified Kohlrausch law of eqn. 1. In practice, such a block-shaped discontinuity can show a totally different character. It can be considered as a combination of two leading–terminating systems, with opposite behaviour. For example, the introduction of 0.012 *M* histidine formate at pH 4.8 in a background electrolyte of 0.01 *M* histidine formate at pH 3.25 is the combination of the systems from Fig. 15C and D. It can be expected that in front of the discontinuity a diffuse zone at higher concentration is formed and at the rear side a sharp zone at lower concentration. To study this behaviour, a long block-shaped zone (50-s pressure injection) of 0.012 *M* histidine formate at pH 4.8 was injected in the background electrolyte 0.01 *M* histidine formate at pH 3.25 in such a way that this discontinuity was introduced at various distances from the detector. In this way several intermediate stages in the separation procedure can be observed. In Fig. 16 the measured electropherograms obtained in this way are given. In Fig. 16A the discontinuity was introduced just before the detector, whereas the distance to the detector increases from Fig. 16A to D. In Fig. 16A the formation of a diffuse zone with a higher UV absorbance than that of the original 0.012 *M* histidine formate solution starts, whereas at the rear side a large, sharp dip is present. From the UV absorbance it can be deduced that the concentration in the dip is about 0.006 *M*. For longer separation times (Fig. 16B and C) the fronting zone increases in height, the original 0.012 *M* zone disappears and the dip elongates. In Fig. 16D the fronting diffuse zone separates

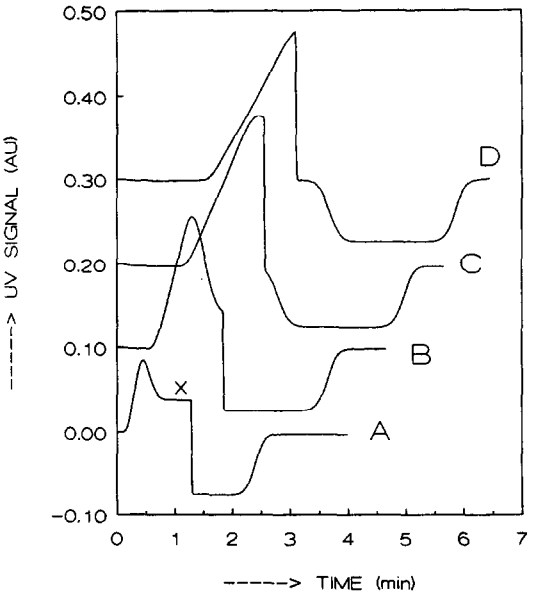

Fig. 16. Electropherograms for 50-s pressure injection of 0.012 *M* histidine formate at pH 4.8 in a background electrolyte of 0.01 *M* histidine formate at pH 3.25. The distance between the injected solution of 0.012 *M* histidine formate and the detector increases from A to D. In (A) the original 0.012 *M* histidine formate plug (X) is partially visible. In front of X a moving boundary zone at higher histidine concentration is formed, whereas at the rear side of X a sharp zone at low concentration is formed. Zone X splits into a migrating system peak and a zone at low concentration at the original position of zone X. In (D) zone X has disappeared and the system peak and dip are released.

from the dip. The fronting diffuse zone migrates with a mobility determined by the composition of the background electrolyte whereas the dip remains at the position of the original block-shaped discontinuity and migrates with the velocity of the EOF.

To illustrate some of these effects, in Fig. 17 some electropherograms are shown for the 20-s pressure injections of several block-shaped discontinuities, followed by a 3-s pressure injection of water as EOF marker in a background electrolyte of 0.01 *M* histidine formate at pH 3.25. For the electropherogram in Fig. 17A, 0.012 *M* histidine formate at pH 4.8 was injected. Although a solution at higher histidine concentration (higher UV absorbance) was injected, a dip just before the EOF marker position and a migrating diffuse peak are the result. Even the

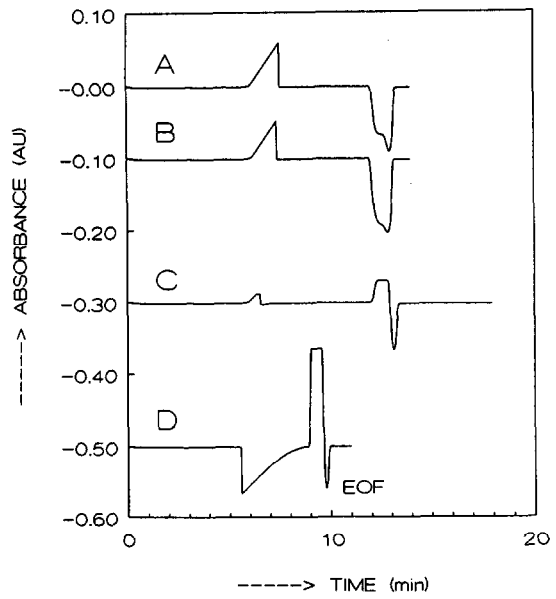

Fig. 17. Electropherograms for 20-s pressure injections of block-shaped discontinuities and 3-s pressure injection of water. The background electrolyte and block-shaped discontinuity were always solutions of histidine formate. The concentration of histidine formate and the pH of the solution for the background electrolytes were respectively (A, B and C) 0.01 *M* and pH 3.25 and (D) 0.01 *M* and pH 4.8 and for the discontinuity (A) 0.012 *M* and pH 4.8, (B) 0.01 *M* and pH 4.8, (C) 0.012 *M* and pH 3.25 and (D) 0.01 *M* and pH 3.25. In all systems system peaks were present.

introduction of 0.01 *M* histidine formate at pH 4.8, where a straight baseline could be expected, results in a positive system peak and a dip just before the EOF dip (Fig. 17B). On injecting a 0.012 *M* solution at pH 3.25, the supply of histidine from the discontinuity is smaller and at the EOF marker position a positive peak remains, but a small positive system peak migrates through the system (Fig. 17C). In Fig. 17D the leading electrolyte was 0.01 *M* histidine formate at pH 4.8 and the discontinuity was 0.01 *M* histidine formate at pH 3.25. Although a straight baseline could be expected, the electropherogram shows a large migrating diffuse dip and a large positive peak at the EOF marker position.

From all these experiments, it can be concluded that the introduction of discontinuities in zone electrophoresis can result in system peaks, with a mobility determined by the background electrolyte.

CONCLUSIONS

Non-steady-state processes in capillary electrophoresis can be estimated with a steady-state mathematical model. Calculations with a steady-state model indicate that in CZE, moving boundary zones can be created by the presence of discontinuities in concentrations of the co-ions and/or pH of the background electrolyte.

The moving boundary zones migrate with a mobility determined by the composition and pH of that background electrolyte, *i.e.*, the ω value of Kohlrausch's regulating function according to eqn. 1 is not locally invariant with time. If the concentration in the moving boundary zone is lower than that of the background electrolyte (negative disturbance), the local E is higher than that of the background electrolyte, through which the zone boundary is sharp. If the concentration is higher than that of the background electrolyte (positive disturbance), the zone is diffuse owing to the fact that the lower concentrations of the zone migrate at a higher mobility than the increasing concentrations of the diffuse zone. Block-shaped discontinuities in pH and/or concentration of the co-ions split up in a migrating part with a velocity determined by the background electrolyte composition and a part migrating with the velocity of the EOF.

To illustrate all these effects, in Fig. 18 the electropherograms are given for 3-s pressure injections of (1) water, (2) a solution of 0.01 *M* histidine adjusted to pH 5 by adding formic acid, (3) a solution of 0.02 *M* KCl and (4) applying a terminating electrolyte of 0.01 *M* histidine formate at pH 5, applying a leading electrolyte of 0.006 *M* histidine adjusted to pH (A) 6 and (B) 4 by adding formic acid. The mobilities of the concentration disturbances are nearly zero at pH 6. For this reason, no special effects can be observed in the electropherograms in Fig. 18A. In electropherogram 1, the EOF peak is present. In electropherogram 2 a positive peak is present at the EOF position, because owing to Kohlrausch's law the initial ω value is high. In electropherogram 3 a negative peak of potassium is present (indirect UV mode), whereas at the EOF position a positive peak is present because the histidine concentration is adapted to the

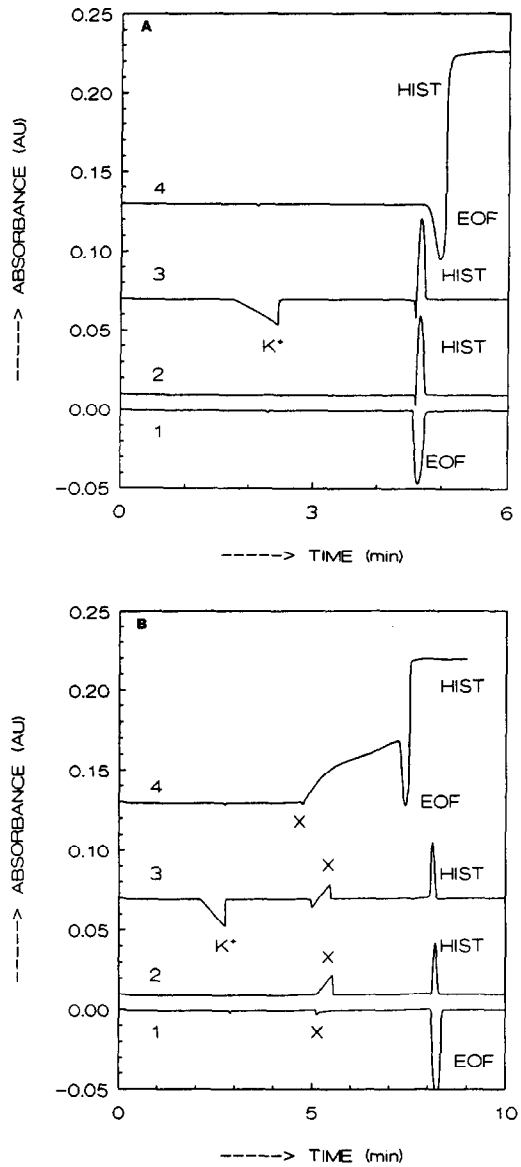

Fig. 18. Electropherograms for the separations of 3-s pressure injections of (1) water, (2) 0.01 *M* histidine adjusted to pH 5 by adding formic acid, (3) 0.02 *M* KCl and (4) the application of a terminating solution of 0.01 *M* histidine formate at pH 5 applying a background electrolyte of 0.006 *M* histidine adjusted to pH (A) 6 and (B) 4 by adding formic acid.

original ω value of the KCl solution. In electropherogram 4 a strong shift in the UV signal is present after the EOF dip due to the migration of the original terminating solution at a higher histidine concentration than the background electrolyte (note that the baseline UV signal is constant before the EOF dip). In Fig. 18B some typical effects are visible on applying a background electrolyte at low pH. In electropherogram 1, the EOF peak splits and a system peak X occurs. In electropherogram 2, a solution of high histidine concentration (positive disturbance) is injected and this peak splits, giving a positive peak X just beginning at the same position of the negative peak in electropherogram 1. The resulting peak at the position of the EOF is smaller than that of the corresponding peak in Fig. 18A. On injecting a 0.02 *M* KCl solution the potassium peak can be observed, a histidine peak at the position of the EOF according to Kohlrausch's law and a system peak X, consisting of a small negative dip followed by a positive peak. This system peak can be explained as follows. In the first instance the KCl solution migrates from the EOF position. According to Kohlrausch's law, the EOF position will be filled with histidine (at a high concentration). Because this process lasts for some time, in the first instance a negative disturbance migrates through the system, followed by the positive disturbance. According to the mathematical model the mobility of the negative disturbance is higher than that of the positive disturbance and migrates with a sharp front. Because the supply of histidine from the terminating solution is small, the positive peak has a limited length. If the terminating electrolyte has a much higher concentration of histidine and the supply from the terminating electrolyte is high (electropherogram 4), a continuous shift of baseline UV signal is obtained. Kohlrausch's law is not valid, showing that this law must not be applied at low pH.

The character of the different kinds of moving boundary zones and their effects on systems peaks and separations is under investigation.

REFERENCES

1 F. Foret, E. Szoko and B.L. Karger, *J. Chromatogr.*, 608 (1992) 3.
2 C. Schwer and F. Lottspeich, *J. Chromatogr.*, 623 (1992) 345.
3 J.L. Beckers, *J. Chromatogr.*, 641 (1993) 363.
4 A. Vinther, F.M. Everaerts and H. Søberg, *J. High Resolut. Chromatogr.*, 13 (1990) 639.

5 J.L. Beckers and M.T. Ackermans, *J. Chromatogr.*, 629 (1993) 371.
6 P. Bocek, P. Gebauer and M. Deml, *J. Chromatogr.*, 217 (1981) 209.
7 P. Bocek, P. Gebauer and M. Deml, *J. Chromatogr.*, 219 (1981) 21.
8 J.L. Beckers and F.M. Everaerts, *J. Chromatogr.*, 480 (1989) 69.
9 F. Kohlrausch, *Ann. Phys. (Leipzig)*, 62 (1897) 209.
10 E.B. Dismukes and R.A. Alberty, *J. Am. Chem. Soc.*, 76 (1954) 191.
11 F.E.P. Mikkers, *Thesis*, University of Technology, Eindhoven, 1980.